Scanning Tunneling Microscopy of Ordered Graphite and Glassy Carbon Surfaces: Electronic Control of Quinone Adsorption

Mark T. McDermott† and Richard L. McCreery*

Department of Chemistry, The Ohio State University, 120 West 18th Avenue, Columbus, Ohio 43210

Received November 15, 1993. In Final Form: July 18, 1994®

Adsorption was examined on STM-characterized graphite and glassy carbon surfaces, in order to relate adsorption behavior to specific surface structures. The adsorption of four electroactive quinones was determined voltammetrically on highly ordered pyrolytic graphite (HOPG) and fractured glassy carbon (GC). The average surface coverage on HOPG was 0.25–0.50, while that on GC was 2.7–4.0, consistent with GC surface roughness. STM of a large number of defects on HOPG yielded an average defect coverage of 0.01 ± 0.004, much too low to account for the observed adsorption by a simple geometric model. STM and adsorption measurements on identical HOPG surfaces showed that adsorption tracks observed defect area, but with the adsorption about 30 times higher than expected. High-resolution STM of HOPG revealed an electronic perturbation near the step defects which was larger than the defect itself by a factor of about 8. The results are consistent with quinone adsorption to the entire electronically perturbed region rather than to only the physical defect. The results are inconsistent with an adsorption mechanism based on specific chemical sites such as oxides or surface radicals. The results imply that adsorption of quinones on GC and defective HOPG depends on an electronic effect such as an electrostatic attraction between the adsorbate and partial surface charges, rather than a specific chemical effect.

Introduction

Our laboratory has examined the basal plane of highly oriented pyrolytic graphite (HOPG) as a structurally well-defined model for more disordered and common carbon materials.[1] HOPG has been investigated previously by Yeager et al.[2] and Gerischer et al.,[3] who observed anomalously low electrode capacitance and attributed it to the electronic properties of the material. We have reported very low electron transfer rates on HOPG compared to glassy carbon (GC) for 18 outer-sphere redox systems.[1e,4] Both the low capacitance[2,3] and slow kinetics[1e,4] at HOPG have been attributed to the semimetal character of ordered graphite, particularly the low density of electronic states (DOS) near the Fermi level.[5] Both the DOS and charge carrier density are 2 or more orders of magnitude lower on HOPG compared to metals,[5,6] resulting in a space charge capacitance and nonselective reduction in electron transfer rates.

A crucial consideration in the study of electrochemistry at HOPG is the role of surface defects.[1c-e] Such defects are well known from scanning tunneling microscopy (STM) of HOPG,[7] with a typical rate of occurrence of 1–10% (stated as the ratio of defect area to projected area).[7d] Given the substantial geometric, electronic, and possibly chemical differences between basal and edge plane graphite, one would expect major differences in reactivity. The double-layer capacitance (C^0), electron transfer rate constant (k^0), and amount of quinone adsorption (Γ) measured on the same basal plane HOPG surface correlated with each other, from which we inferred that all three track defect density.[1d] Furthermore, the observed k^0 is extremely sensitive to the presence of defects because they appear to be sites of more facile electron transfer compared to the pristine basal plane.[1] This may be due to the presence of a specific chemical functionality or to some other disorder-induced phenomenon at HOPG surface defects. The correlation of anthraquinone-2,6-disulfonate (2,6-AQDS) adsorption with disorder also implies a dependence of adsorption on defect density. For example, 2,6-AQDS adsorbs at GC electrodes, yielding a saturation coverage of >200 pmol/cm^2, yet its adsorption on low-defect HOPG is below the voltammetric detection limit (<1 pmol/cm^2).[1d]

In a more general context, these observations bear on the question of reactive sites on carbon electrodes. If kinetics and adsorption depend on specific chemical sites, these sites may exist only at defects on HOPG electrodes. Alternatively, defects or disorder may change the electronic properties of the electrode, thus affecting electrochemical behavior. For example, as observed with ordered

* Author to whom correspondence should be addressed.

† Present address: Department of Chemistry and Ames Laboratory, USDOE, Iowa State University, Ames, IA 50011.

® Abstract published in *Advance ACS Abstracts,* October 15, 1994.

(1) (a) Bowling, R.; Packard, R.; McCreery, R. L. *J. Am. Chem. Soc.* **1989,** *111,* 1217. (b) Rice, R. J.; McCreery, R. L. *Anal. Chem.* **1989,** *61,* 1638. (c) Robinson, R. S.; Sternitzke, K.; McDermott, M. T.; McCreery, R. L. *J. Electrochem. Soc.* **1991,** *138,* 2454. (d) McDermott, M. T.; Kneten, K. R.; McCreery R. L. *J. Phys. Chem.* **1992,** *96,* 3124. (e) Kneten, K. R.; McCreery, R. L. *Anal. Chem.* **1992,** *64,* 2518.

(2) (a) Randin, J. P.; Yeager, E. J. *Electrochem. Soc.* **1971,** *118,* 711. (b) Morcos, I.; Yeager, E. *Electrochim. Acta* **1972,** *15,* 257. (c) Randin, J. P.; Yeager, E. *J. Electroanal. Chem.* **1972,** *36,* 257. (d) Randin, J. P.; Yeager, E. *J. Electroanal. Chem.* **1975,** *58,* 313.

(3) (a) Gerischer, H. *J. Phys. Chem.* **1985,** *89,* 4249. (b) Gerischer, H.; McIntyre, R.; Scherson, D.; Storck, W. J. *J. Phys. Chem.* **1987,** *91,* 1930. (c) McIntryre, R.; Scherson, D.; Storch, W.; Gerischer, H. *Electrochim. Acta* **1987,** *32,* 51.

(4) Cline, K. K.; McDermott, M. T.; McCreery, R. L. *J. Phys. Chem.* **1994,** *98,* 5314.

(5) (a) Spain, I. T. In *Chemistry and Physics of Carbon*; Walker, P. L., Jr., Thrower, P. A., Eds.; Marcel Dekker: New York, 1973; Vol. 8, pp 1–150. (b) Spain, I. T. In *Chemistry and Physics of Carbon*; Walker, P. L., Thrower, P. A., Eds.; Marcel Dekker: New York, 1980; Vol. 16, pp 119–304.

(6) (a) Kittel, C. *Introduction to Solid State Physics,* 6th ed.; Wiley: New York, 1986; p 134. (b) Kokko, K.; Ojala, E.; Mansikka K. *Phys. Status Solidi B* **1989,** *153,* 235.

(7) See for example: (a) Fuchs, H. *Fresenius' Z. Anal. Chem.* **1987,** *329,* 113. (b) Rabe, J. P.; Sano, M.; Batchelder, D.; Kalatchev, A. A. *J. Microsc.* **1988,** *152,* 573. (c) Snyder, S. R.; White, H. S.; Lopez, S.; Abruna, H. D. *J. Am. Chem. Soc.* **1990,** *112,* 1333. (d) Chang, H.; Bard, A. J. *Langmuir* **1991,** *7,* 1143. (e) Clemmer, C. R.; Beebe, T. P. *Science* **1991,** *251,* 640. (f) Siperko, L. M. *J. Vac. Sci. Technol. B* **1991,** *9,* 1061. (g) Snyder, S. R.; Foecke, T.; White, H. S.; Gerberich, W. W. *J. Mater. Res.* **1992,** *7,* 341.

0743-7463/94/2410-4307$04.50/0

semiconductors, disorder of the HOPG surface structure may generate localized electronic states which increase the DOS near the Fermi level,[5b] thus making electron transfer more favorable. For the case of electron transfer to outer-sphere redox systems at HOPG electrodes, we concluded that the electronic factor is more important than specific chemical sites.[4]

So far, the influence of surface defects on electrochemical observables such as k^0, C^0, and Γ has been derived through correlation (eg. k^0 vs Γ and C^0 vs Γ) without explicit consideration of surface defect structure.[1d] The current report involves direct characterization of HOPG defects with STM at low and high resolution. The STM observable structure is then quantitatively compared to quinone adsorption. GC electrodes, which provide a basis for the behavior of disordered carbon surfaces, are also examined in this manner. The results provide insight into the mechanism of adsorption and electron transfer and bring up some interesting questions concerning the nature of "active sites" at carbon electrodes.

Experimental Section

Unless noted otherwise, "HOPG" refers to the basal plane of cleaved highly oriented pyrolytic graphite (obtained as a gift from Dr. Arthur Moore, Union Carbide, Parma, OH). HOPG electrodes were cleaved by peeling with adhesive tape. Glassy carbon (GC-20) electrodes were obtained from Tokai and were cut either from a 2 mm thick plate or from a 3 mm diameter rod. The microrods (approximately 0.5 × 0.5 mm cross section) cut from the GC plate were embedded in epoxy (Eccobond 55, Emerson and Cummings Inc, Woburn, MA) and used for the electrochemical experiments. Fracturing procedures were as described previously.[16] The 3 mm rods were utilized for STM imaging because of the ease of mounting and lack of sample tilt compared to the microrods.[16e] No differences were observed in STM images between the 3 mm rods and the microrods.

All solutions were prepared with water purified by reverse osmosis and deionized with a NANOPure II (Barnstead, Dubuque, IA) water purification system. Solutions were degassed prior to usage with purified argon. Disodium anthraquinone-1,5-disulfonate (1,5-AQDS), disodium anthraquinone-2,6-disulfonate (2,6-AQDS), monosodium anthraquinone-2-disulfonate (AQMS), and phenanthrenequinone (PQ) were obtained from Aldrich (Milwaukee, WI). 2,6-AQDS was recrystallized twice from deionized water, PQ was recrystallized from benzene, and 1,5-AQDS and AQMS were used as received. 10^{-5} M solutions of quinones in 0.1 M $HClO_4$ (Baker, Phillipsburg, NJ) degrade after 2–3 days and were prepared accordingly.

Electrochemical experiments at HOPG electrodes were carried out in an inverted drop cell (IDC) as described previously.[1d,e] Electrode areas were determined in 1 mM $K_4Fe(CN)_6$ (Baker) in 1.0 M KCl (Jenneile Chemical, Cincinnati, OH) via chronoamperometry. The average electrode area was 0.20 ± 0.03 cm^2 ($N = 20$). Electrochemical experiments at GC electrodes were carried out in a Teflon cell.

Cyclic voltammetric waveform inputs were generated by a function generator (Tektronix) triggered by a Labmaster A/D board (Scientific Solutions). The potential application to the cell and current measurement was carried out via a custom-built potentiostat (Advanced Idea Mechanics, Columbus, OH). E vs t and i vs t waveforms were collected and transferred to a PC by the A/D board and custom software.[8] Chronoamperometric potential steps were also generated by the A/D board and custom software.

Adsorption of quinones was quantified by measuring the baseline-corrected area under the voltammetric reduction wave and applying the equation $Q = nFA\Gamma$,[9] where Q is the charge under the voltammetric wave, n is the number of electrons ($n = 2$), F is Faraday's constant, A is the electrode area, and Γ is the amount of surface bound quinone (reported in pmol/cm^2).

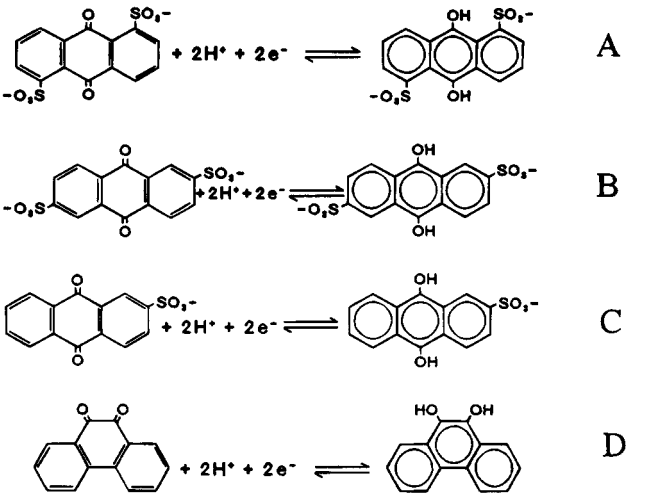

Figure 1. Structures and electrode reactions (acid solution) of the four quinones studied: (A) 1,5-AQDS, (B) 2,6-AQDS, (C) AQMS, (D) PQ.

Adsorption was monitored with time until a constant value was observed (~30 s).

STM images were obtained with a commercial Nanoscope II (Digital Instruments, Santa Barbara, CA). Images shown here were obtained in ambient air. In addition, some images which were analyzed but not shown were obtained in 0.1 M $HClO_4$. All images shown for HOPG are unfiltered and were obtained in the constant current mode at scan rates less than 10 Hz. Parameters for GC images are listed in the figure captions. Bias voltage and tunneling current are listed in the caption of each figure.

Tunneling tips were prepared by electrochemically etching tungsten rods (0.010 in. diameter, FHC, Brunswick, ME) at 30 V rms in 1.5 M KOH. All tips used in this work were able to image the normal basal plane atomic structure on HOPG, characterized by 0.25 nm periodicity,[10] when imaging was done away from defects.

Results

We have previously characterized the adsorption of 2,6-AQDS at carbon electrodes.[1d] The adsorption of 2,6-AQDS at GC and laser-damaged HOPG is described by a Langmuir isotherm and reaches saturation coverage at solution concentrations less than 10^{-6} M. In addition, it was shown that the observed quantity of adsorbed 2,6-AQDS, Γ_{obs}, tracked the density of surface defects at cleaved HOPG electrodes. In order to show that this behavior is not unique to 2,6-AQDS, the adsorption of three similar quinone species has been examined. The structures of these systems as well as their redox reactions in acid solutions (pH ~ 1) are shown in Figure 1. Brown and Anson have demonstrated that phenanthrenequinone (PQ, Figure 1D) and anthraquinone-2-monosulfonate (AQMS, Figure 1C) strongly adsorb at pyrolytic graphite (PG) electrodes and reach saturation coverage at solution concentrations of 10^{-6} M.[9,11] Recently, anthraquinone-1,5-disulfonate (1,5-AQDS, Figure 1A) has been shown to behave similarly at PG.[12] Thus, all four quinone systems adsorb strongly on disordered carbon surfaces such as PG and GC.

Voltammograms of 10^{-5} M solutions of each quinone at cleaved HOPG are shown in Figure 2. At this solution concentration, the Faradaic current due to diffusion is too low to observe and all observable current above back-

(8) Sternitzke, K. D. Ph.D. Dissertation, The Ohio State University, 1990.
(9) Brown, A. P.; Anson, F. C. *Anal. Chem.* **1977**, *49*, 1589.
(10) Heben, M. J.; Dovek, M. M.; Lewis, N. S.; Penner, R. M.; Quate, C. F. *J. Microsc.* **1988**, *152*, 651.
(11) Brown A. P.; Koval C.; Anson, F. C. *J. Electroanal. Chem.* **1976**, *72*, 379.
(12) Zhang, J.; Anson, F. C. *J. Electroanal. Chem.* **1991**, *331*, 945.

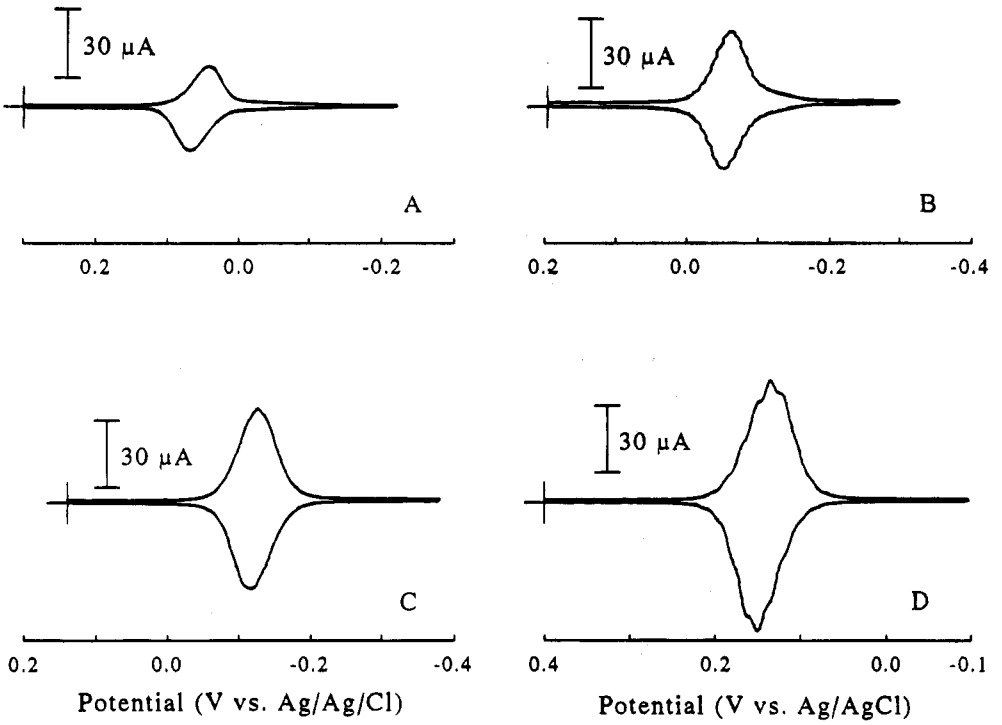

Figure 2. Cyclic voltammograms of four quinones at cleaved HOPG electrodes. In all cases solution concentration was 10^{-5} M in 0.1 M $HClO_4$ and $\nu = 1.0$ V/s. (A) 1,5-AQDS, $\Gamma_{obs} = 25$ pmol/cm^2. (B) 2,6-AQDS, $\Gamma_{obs} = 49$ pmol/cm^2. (C) AQMS, $\Gamma_{obs} = 65$ pmol/cm^2. (D) PQ, $\Gamma_{obs} = 86$ pmol/cm^2.

Table 1. Adsorption Data for Four Adsorbates at Cleaved Basal Plane HOPG Electrodes

adsorbate	area[a] (Å^2)	Γ_{sat}[b] (pmol/cm^2)	Γ_{obs} (pmol/cm^2)	Θ_{obs}[c]	N[d]
1,5-AQDS	138	120	27 ± 8	0.23 ± 0.07	6
2,6-AQDS	126	132	45 ± 13	0.31 ± 0.10	11
AQMS	111	150	65 ± 12	0.43 ± 0.08	7
PQ	94	177	86 ± 12	0.49 ± 0.07	6

[a] Theoretical molecular area assuming a flat orientation. [b] Theoretical monolayer for flat surface and flat adsorption orientation. [c] Observed fractional coverage, $\Gamma_{obs}/\Gamma_{sat}$. [d] Number of HOPG surfaces examined.

ground is due to adsorbed quinone.[13] The peak width of the voltammograms as well as the proportionality between scan rate and peak current indicate that all quinone systems are well-behaved surface-bound redox species at HOPG electrodes and exhibit qualitatively similar voltammetry.[14]

Quantitative adsorption results on several cleaved HOPG surfaces are shown in Table 1. The theoretical molecular area and saturation coverage, Γ_{sat}, were calculated from the van der Waals radii by the method of Hubbard,[15] for the case of flat orientation. Θ_{obs} is defined as $\Gamma_{obs}/\Gamma_{sat}$ and represents the fraction of the theoretical monolayer adsorbed. In Table 1 the relative standard deviation of Θ_{obs} is fairly high (15−30%) because of cleave-to-cleave variation in defect density. However, all four molecules exhibit Θ_{obs} in the range of 0.23−0.49 at HOPG. It should be stressed at this point that Table 1 lists average Γ values, with a few individual values on very low defect surfaces exhibiting the very low adsorption (<1 pmol/cm^2) reported previously.[1d]

Table 2. Adsorption Data for Four Adsorbates at Fractured GC Electrodes

adsorbate	Γ_{obs} (pmol/cm^2)	Θ_{obs}	N
1,5-AQDS	430 ± 75	3.6 ± 0.6	3
2,6-AQDS	530 ± 50	4.0 ± 0.4	5
AQMS	450 ± 50	3.0 ± 0.4	3
PQ	470 ± 80	2.7 ± 0.5	3

For comparison, the adsorption of the four quinone systems in Figure 1 was also examined at fractured GC electrodes.[16] Quinone voltammetry at fractured GC is qualitatively similar to that observed at HOPG; however, the amount of surface-bound quinone varied between 430 and 530 pmol cm^2, corresponding to 2.7−4.0 apparent monolayers. We have shown by STM analysis that fractured GC is much rougher than HOPG or even polished GC.[16e] From the data listed in Tables 1 and 2, it is clear that the average quantity of adsorbed quinone is much less at HOPG electrodes (<0.5 monolayer) compared to GC (≥1 monolayer). In addition, greater-than-monolayer coverage is always observed at fractured GC while in some cases HOPG exhibits negligible adsorption.

With reference to the data in Table 1, the average θ_{obs} is no less than 0.23 at HOPG electrodes for any of the adsorbates studied. The defect area reported from STM analysis of cleaved HOPG is 0.01−0.10,[7d] significantly lower than θ_{obs}. As elaborated below, this discrepancy implies that a model based on quinone adsorption only to STM-observable defects is quantitatively inconsistent with the observations.

Figure 3A is a 12 × 12 μm STM image of a typical HOPG surface used in this study. This image is qualitatively

(13) Bard, A. J.; Faulkner, L. R. *Electrochemical Methods*; Wiley: New York, 1980.

(14) At long times (>3 min) the voltammetry of 1,5-AQDS displays a second wave at ~0.03 V vs Ag/AgCl. This is consistent with the observations of Zhang and Anson,[12] who attributed this second wave to a change in adsorption orientation from flat to edgewise. Γ_{obs} for 1,5-AQDS was always measured within 1 min of solution exposure to the electrode, before this second voltammetric wave developed.

(15) Soriaga, M. P.; Hubbard, A. T. *J. Am. Chem. Soc.* **1982**, *104*, 2735.

(16) (a) Rice, R.; Allred, C.; McCreery, R. L. *J. Electroanal. Chem.* **1989**, *263*, 163. (b) Rice, R. J.; Pontikos, N. M.; McCreery, R. L. *J. Am. Chem. Soc.* **1990**, *112*, 4617. (c) Allred, C. D.; McCreery, R. L. *Anal. Chem.* **1992**, *64*, 444. (d) Pontikos, N. M.; McCreery, R. L. *J. Electroanal. Chem.* **1992**, *324*, 229. (e) McDermott, M. T.; McDermott, C. A.; McCreery, R. L. *Anal. Chem.* **1993**, *65*, 937.

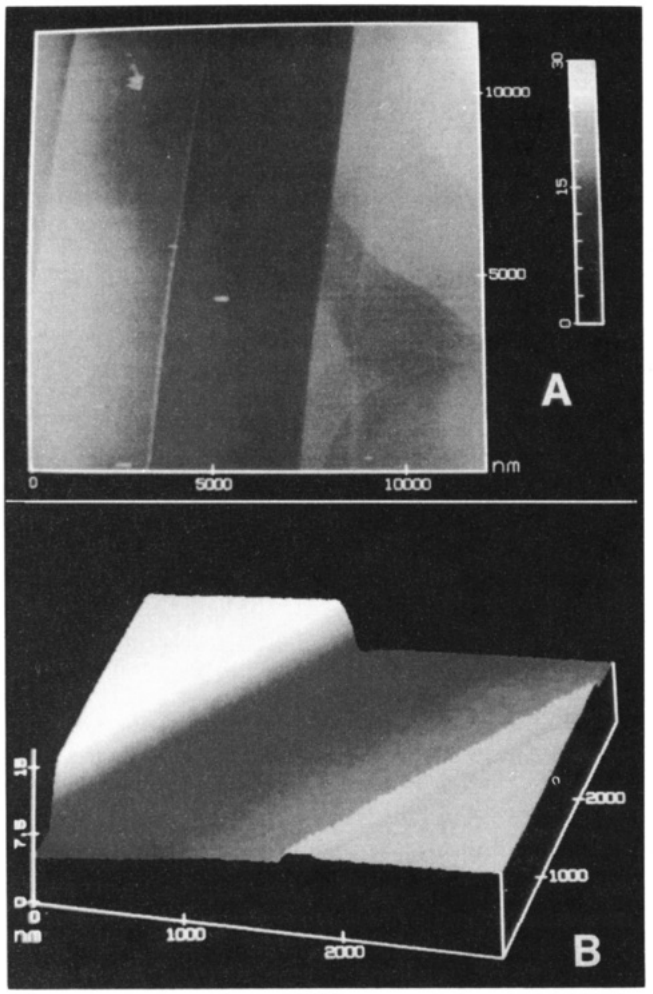

Figure 3. Low-resolution STM images of cleaved HOPG. For both images, $V_b = 20$ mV and $i_t = 2$ nA. (A) 12×12 μm top view image, z-scale = 0−30 nm. (B) 3×3 μm surface plot image, z-scale = 0−15 nm.

representative of 65 low-resolution images obtained which revealed defects similar to those cataloged by Chang and Bard.[7d] The large majority of defects (>90%) are step edges, the heights of which are predominantly multiples of the graphitic interplane spacing, 0.335 nm.[17-19] Thus, it is likely that the "face" of the step defects is composed of graphitic edges. Because most of these steps are parallel to the direction of the cleave, they probably result from the cleavage process.[7d] The curved defects apparent in Figure 3A were observed occasionally but were rare compared to straight step edges. Examples of step defects with heights of 5.0 nm (~15 graphitic layers) and 1.3 nm (4 layers) are shown in Figure 3B. A statistical study of 65 12×12 μm images of nine cleaved HOPG surfaces is summarized in Table 3. The 518 step edge defects observed varied in height with the majority of the steps being 1−3 layers high. It should be pointed out that these observations depend on the HOPG grade, sample, and

(17) McCreery, R. L. In *Electroanalytical Chemistry*; Bard, A. J., Ed.; Marcel Dekker: New York, 1991; Vol. 17, pp 221−374 and references therein.

(18) The heights of the steps do not vary with changes in the tunneling gap resistence, R_g, in the range from 10^6 to 10^8 Ω. This indicates that contamination-mediated deformation of the graphite by the STM tip does not influence step heights in a manner analogous to the atomic corrugation.[19]

(19) (a) Coombs, J. H.; Pethica, J. B. *IBM J. Res. Dev.* **1986**, *30*, 455. (b) Solar, J. M.; Baro, A. M.; Garcia, M.; Rohrer, H. *Phys. Rev. Lett.* **1986**, *57*, 444. (c) Mamin, H. J.; Ganz, E.; Abraham, D.; Thomson, R. E.; Clarke, J. *Phys. Rev. B* **1986**, *34*, 9015. (d) Yamada, H.; Fujii, T.; Nakayama, K. *J. Vac. Sci. Technol. A* **1988**, *6(2)*, 293.

Table 3. Height Statistics for 518 Step Defects Examined by STM

step height[a] (nm)	graphitic layers	percentage of 518 defects
0.3	1	11
0.7	2	26
1.0	3	19
1.3	4	9
1.7	5	14
2.0	6	9
2.3	7	5
>2.3	>7	7

[a] The error in the height measurement is ±15% due to piezo calibration error.

Table 4. Area Fraction of Defects for Nine Basal Plane HOPG Electrodes Determined from STM Images

electrode	f_d	N^a
1	0.008 ± 0.001^b	7
2	0.01 ± 0.005	6
3	0.002 ± 0.001	5
4	0.016 ± 0.007	9
5	0.007 ± 0.003	5
6	0.011 ± 0.005	6
7	0.010 ± 0.004	6
8	0.015 ± 0.006	11
9	0.012 ± 0.005	10
total	0.010 ± 0.004	65

[a] N corresponds to the number of 12×12 μm images utilized in the determination of f_d for a particular electrode surface. [b] Standard deviation for N images.

cleaving technique. The samples studied here by STM were the same as those evaluated electrochemically, and in some cases (noted below), the same surface was characterized with both STM and adsorption.

The geometric defect area will be defined here as the area of exposed edge plane at a step defect. For a given step, the defect area is easily calculated as the step height times the step length. The fractional area of defects, f_d, is then defined as the defect area for a given image divided by the projected area of the image, usually 12×12 μm. Note that this definition of f_d is strictly geometric and does not take into account any corrugation of either basal or edge plane. For the nine surfaces summarized in Table 3, f_d is listed in Table 4. For each surface, a number of images (N) were acquired at random locations on the surface, for a total of 65 images and 518 defects. Although the range of f_d is fairly large (0.002−0.016), the overall average for 65 images is 0.010 ± 0.004, which is the lower end of the 1−10% range reported by Chang and Bard.[7d] Stated differently, an average of 1% of a given HOPG surface consists of edge plane, and 99% is perfect basal plane.

Notice that the average f_d determined from STM images ($f_d = 0.010$) is much smaller that the average fractional coverage by the adsorbates listed in Table 1 ($\Theta_{obs} = 0.23$−0.49). Thus far, this comparison is based on averages of a large number of surfaces, since f_d and Θ_{obs} were not determined simultaneously. To confirm the observed difference, f_d and Θ_{obs} were determined on the *same* HOPG surfaces by obtaining STM images immediately after 2,6-AQDS adsorption was measured. 2,6-AQDS was chosen as a representative adsorbate because it has been more thoroughly characterized at HOPG electrodes than the other quinones.[1d] For a given surface, Γ_{obs} was determined first by voltammetry of absorbed 2,6-AQDS. Then the solution was removed and 5−9 12×12 μm STM images were acquired at random positions on the electrode surface. Table 5 compares the average f_d, calculated as before, to Θ_{obs}. As shown graphically in Figure 4, Θ_{obs} tracks f_d, but

Table 5. Correlation between Area Fraction of Defects from STM and Observed Adsorption of 2,6-AQDS at Cleaved Basal Plane HOPG Electrodes

surface	STM f_d	N^a	Γ_{obs} (pmol/cm^2)	Θ_{obs}
1	0.007 ± 0.003	5	31	0.23
2	0.008 ± 0.001	7	34	0.26
3	0.010 ± 0.004	6	44	0.33
4	0.011 ± 0.005	6	49	0.37
5	0.016 ± 0.007	9	65	0.49

[a] Number of 12 × 12 μm images used to determine f_d for the surface.

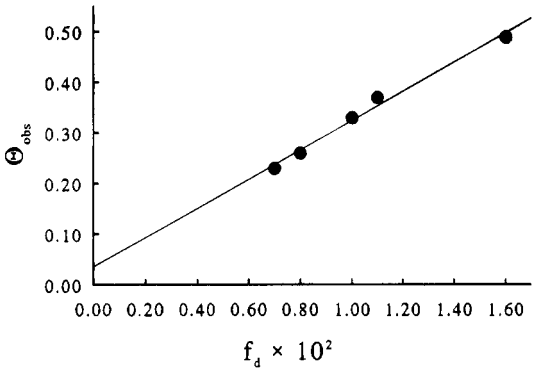

Figure 4. Plot of Θ_{obs} derived from 2,6-AQDS adsorption versus the area fraction of defects determined from STM images at five HOPG electrodes. Line through the points is the linear least-squares fit of the data. See text for equation of line.

with a slope much greater than 1.0. Linear regression of the plot in Figure 4 yields the expression $\Theta_{obs} = 29f_d + 0.03$ ($r = 0.994$). The factor of 29 for the ratio of Θ_{obs} to f_d when both are determined on the same surface (Figure 4) agrees with the factor of 30 observed for the average values of Θ_{obs} for 2,6-AQDS (Table 1) and f_d (Table 4) when obtained on different surfaces.

Table 5 and Figure 4 demonstrate that much more 2,6-AQDS adsorbs to slightly defective HOPG than would be expected if 2,6-AQDS adsorbed only to the geometric edge plane. It is possible that the excess is due to adsorption in an edge orientation rather than flat,[12,15] but this would account for at most a factor of 2. The dimensions of a 2,6-AQDS molecule (ca. 10 × 13 Å) are comparable to the height of a 3–4 layer step edge, so it appears unlikely that the excess is due to a large molecule adsorbing to a small defect. Multilayer adsorption on the defect is possible but was never observed on GC or purposely damaged HOPG.[1d] While these simple explanations could cause a small increase in Θ_{obs} over f_d, they cannot account for a factor of 30. Intercalation in graphite is well known, although generally in nonaqueous solvents or strong aqueous acids.[20] However, intercalation has not been reported for large organic ions and should not be similar for the dianions, monoanions, and neutral species studied here.

Figure 5 shows high-resolution images of a 0.7 nm high (2 layer) step edge at progressively higher magnifications. The 500 × 500 nm image in Figure 5A depicts a well-defined step surrounded by an otherwise perfect basal plane. Figure 5B is a high-resolution scan (7 × 7 nm) showing the step edge in the upper right corner. The region to the right of the step edge in the extreme upper right of the image is the lower terrace. Although not easily seen in Figure 5B, the basal plane of the lower terrace exhibits the expected graphitic order with an atomic spacing of 0.25 nm (see Figure 5C). At a large distance from the step (>5 nm) on the top terrace at the left border of Figure 5B, the same graphitic order is observed. Also, the atomic rows of the lower terrace, which are more apparent in Figure 5C, are in registry with those of the upper terrace at points distant from the step edge. However, within about 2–3 nm to the left of the edge, the image of the upper layer is qualitatively different from that of the normal basal plane observed in either the lower layer or the upper layer far from the edge. In this area, the normal graphitic atomic structure is difficult to distinguish. Also, some atomic positions, corresponding to next-nearest neighbor sites, appear brighter than the surrounding, nearest neighbor sites. Note, for example, the row of bright spots along the direction indicated by the arrow in Figure 5B. The spacing between the apparent maxima along this row is 0.43 nm.

A number of recent studies have reported anomalous perturbations on graphite near defects, an example of which is characterized by a periodicity corresponding to the next-nearest neighbor spacing (i.e. $\sqrt{3} \times \sqrt{3}$) which decays over a distance of a few nanometers.[21] Thus, it is reasonable to assume that the step in Figure 5 is causing some type of perturbation of the STM-observable graphite structure. The extent of this perturbation is more easily seen in the 5 × 5 nm image in Figure 5C. The disturbance of the HOPG structure is readily apparent as an arrangement of very bright spots to the left of the step edge. This apparent increase in the corrugation does not depend on scan direction, sign of the bias voltage, or tunnel gap resistance, R_g, in the range 5×10^6 to 3×10^7 Ω (i.e. the range of R_g in which we observe atomic resolution). These observations provide strong evidence that the increase in brightness near the step is not an imaging artifact (e.g. feedback overshoot) or compression of the graphite by the force exerted by the tip,[18,19] Notice that this distortion exists only on the upper layer and extends many atomic rows away from the defect.

In order to understand the effect of the atomic scale structure of HOPG defects on quinone adsorption, we attempted to directly image adsorbed 2,6-AQDS. For five HOPG surfaces, at which the presence of adsorbate was confirmed by voltammetry, molecular resolution of adsorbed 2,6-AQDS was not unambiguously achieved. However, disorder was observed near defects, and normal graphitic order was apparent on the basal plane far from defects. The inability to directly image adsorbed 2,6-AQDS may be due to interference of the disorder at the defect or thermal- or tip-induced motion of 2,6-AQDS molecules.

Referring to Figure 5C, one can define an approximate boundary between the disturbed periodicity near the step edge and the normal graphite periodicity. In this case, the apparent disrupted region extends about 2.5 nm to the left of the defect. We define the length of the disruption qualitatively as the distance from the step edge to the point on the upper terrace where the normal graphite atomic structure can be observed. Although this value depends on image rendition and an approximate estimate of the perturbation boundary, it is clear that the perturbation is much larger than the step edge height. Table 6 lists the length of this apparent perturbation for 11 step edges examined by high-resolution STM. All 11 defects revealed a structure near the step which did not coincide with the common basal plane order. Four steps exhibited

(20) Alsmeyer, D. C.; McCreery, R. L. *Anal. Chem.* **1992**, *64*, 1528.

(21) (a) Porte, L.; deVilleneuve, C. H.; Phanar, M. *J. Vac. Sci. Technol. B.* **1991**, *9*, 1064. (b) Xhie, J.; Sattler, K.; Muller, U.; Venkateswaran, N.; Raina, G. *J. Vac. Sci. Technol. B.* **1991**, *9*, 1064. (c) Albrecht, T. R.; Mizes, H. A.; Nogami, J.; Park, S. I. *Appl. Phys. Lett.* **1988**, *52*, 362. (d) *Physics Today* **1988**, *41*, 129. (e) Mizes, H. A.; Foster, J. S. *Science* **1989**, *244*, 559. (f) Sattler, K. *J. Int. J. Mod. Phys. B* **1992**, *6*, 3603.

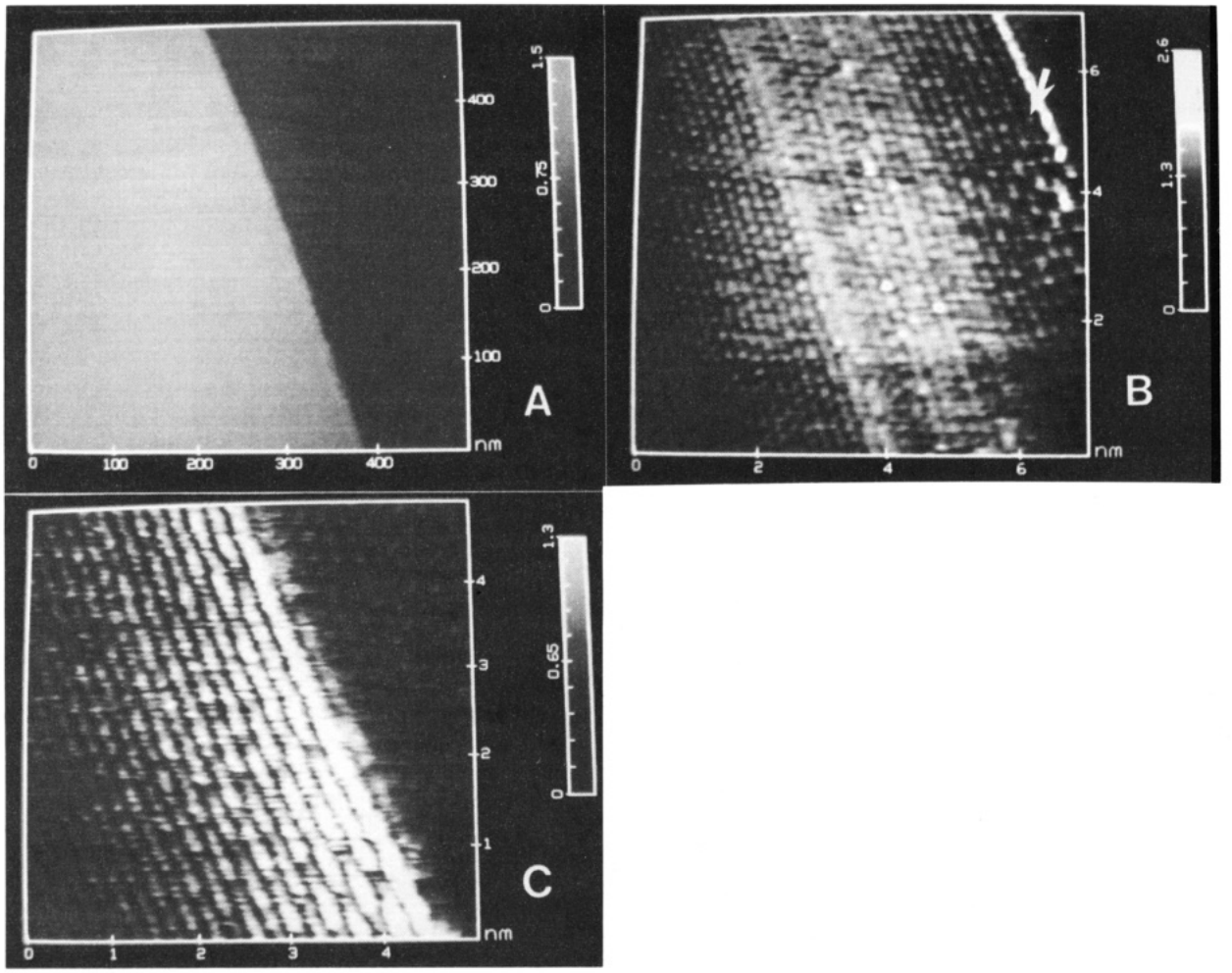

Figure 5. STM images of a HOPG step defect. For all images, $V_b = 20$ mV and $i_t = 2$ nA. (A) 500 × 500 nm image, z-scale = 0−1.5 nm, step height is 0.8 nm. (B) 7 × 7 nm image, z-scale = 0−2.6 nm. The arrow indicates a row of apparent maxima exhibiting a periodicity of 0.43 nm. (C) 5 × 5 nm image, z-scale = 1.3 nm.

Table 6. Correlation between Step Defect Height and Disorder Width at Cleaved Basal Plane HOPG Electrodes

step height (nm)	graphite layers	disorder length (nm)	disorder length/step height
0.3	1	1.5	5.0
0.3	1	2.0	6.7
0.3	1	2.5	8.3
0.7	2	3.0	4.3
0.7	2	5.0	7.1
0.7	2	7.0	10
1.0	3	9.0	9
1.4	4	15	9.1
1.7	5	15	8.8
3.0	9	28	9.3
100	30	85	8.5
			7.8 ± 1.8 ($N = 11$)

the large periodicity shown in Figure 5C. In the other cases, a highly disordered structure, characterized by no apparent periodicity and large corrugation, was observed. It is clear from Table 6 that the perturbation is more extensive for higher steps. The ratio of the disorder length away from the step to the step height varies from 5.0 to 9.3 but shows no trend with step height. The average ratio is 7.8 ± 1.8 for 11 steps.

From the results presented above, it is clear that the STM observable HOPG surface structure near defects is disordered. It is well known that GC exhibits a much more disordered bulk structure than HOPG.[17] We therefore examined the surface of fractured GC with STM in order to investigate the atomic scale structure of a disordered carbon surface and compare with our observations at HOPG defects.

Figure 6 shows STM images of a fractured GC electrode surface. Figure 6A,B shows lower resolution images which display the rough, nodular surface structure characteristic of fractured GC.[16d,e] Figure 6C,D shows representative atomic scale images containing limited areas of periodicity. The observation of periodicity indicates order; however, only ~45% of high-resolution images of six different GC electrodes revealed regions of order which occupied <10% of the total area imaged at high resolution (38 5 × 5 nm images). Stated differently, 90% of the fractured GC surface structure contains no STM-recognizable order, which is illustrated in the area surrounding the ordered regions in Figure 6C,D.

The ordered regions seen at fractured GC (Figure 6C,D) exhibit a periodicity of 0.29 ± 0.01 nm; however, a hexagonal structure typical of HOPG was never observed. It is apparent that the STM observable atomic structure of GC is highly disordered compared to basal plane HOPG. Recall from Table 2 that quinones adsorb at monolayer coverage at GC electrodes.

Discussion

For the average values of both θ_{obs} and f_d for a large number of HOPG defects and the same quantities measured on identical HOPG surfaces, the adsorption of quinones exceeds the geometric area of the graphitic edge plane by a factor of 30. This factor is much too large to be caused by adsorption orientation, and multilayer

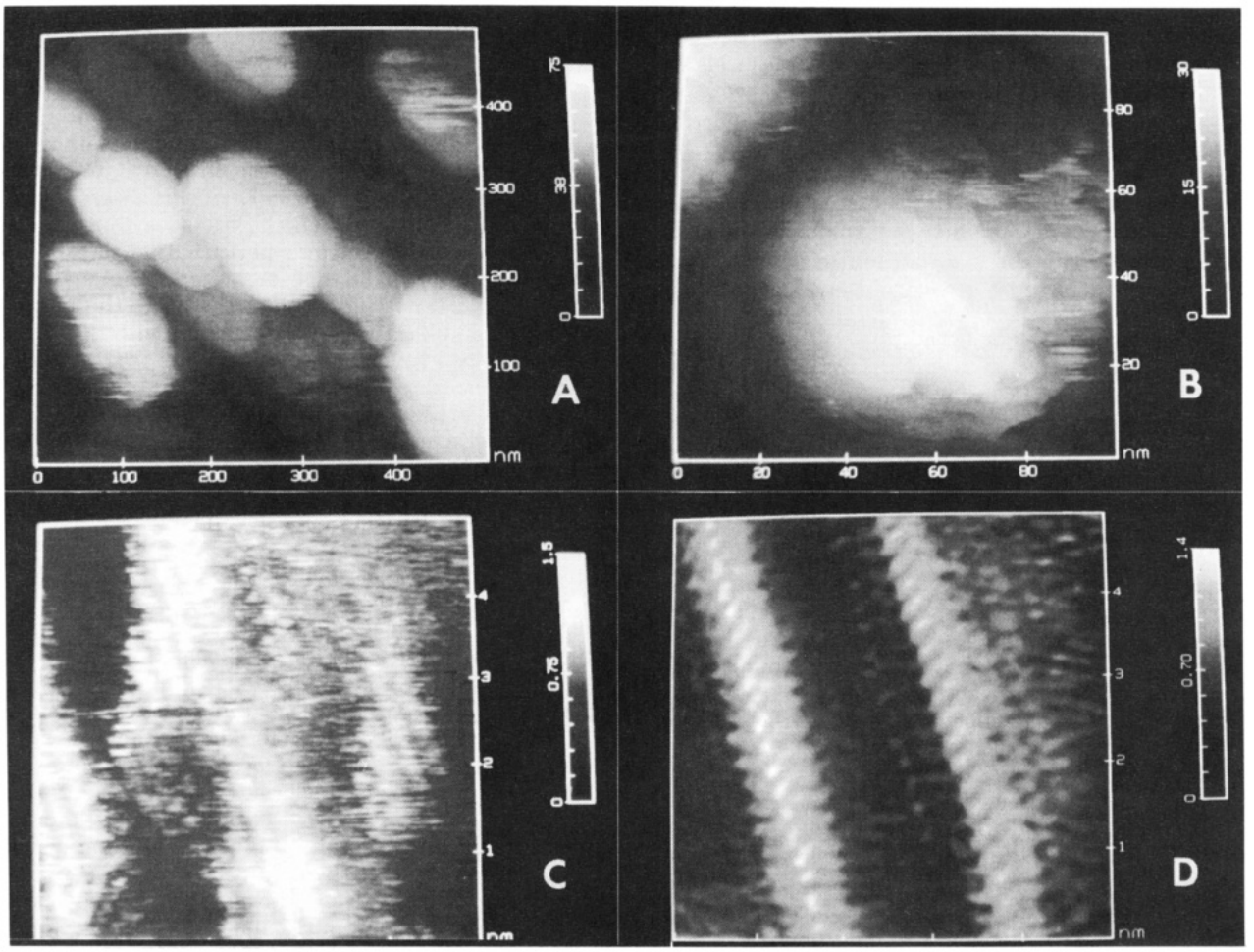

Figure 6. STM images of fractured GC. (A) 500 × 500 nm raw data, constant current image, $V_b = 500$ mV and $i_t = 0.5$ nA, z-scale = 0−75 nm. (B) 100 × 100 nm raw data, constant current image, $V_b = 500$ mV and $i_t = 0.5$ nA, z-scale = 0−30 nm. (C) 5 × 5 nm low pass filtered, constant height image, $V_b = 200$ mV and $i_t = 0.5$ nA, z-scale = 0−1.5 nm. (D) 5 × 5 nm low pass filtered, constant height image, $V_b = 200$ mV and $i_t = 0.5$ nA, z-scale = 0−1.4 nm.

adsorption or intercalation is unlikely. When adsorption mechanisms of quinones in graphitic carbon are considered, several possibilities involve specific interactions with surface functional groups.[22,23] Specific chemical interactions such as covalent or ionic bonding to functional groups would be limited to edge sites and should yield θ_{obs} comparable to or less than f_d. The large discrepancy between θ_{obs} and f_d for HOPG rules out quinone adsorption to specific sites.

Nonspecific adsorption interactions include dispersion interactions such as London and van der Waals forces, interactions between permanent dipoles, and hydrophobic effects. As noted by Arnett et al., the adsorption enthalpy for a variety of adsorbates on polycrystalline graphite tracked the polarizability of the adsorbate and did not depend on the presence of particular functional groups. They concluded that adsorption was mediated by dispersion interactions.[23] Chen and McGuffin[24] observed interactions between pyrene and polar solvent molecules and concluded that partial charges on the carbon atoms in pyrene resulted in electrostatic attraction to polar molecules. Newcomb and Gellman[25] concluded that attractive interactions between partial charges in aromatic systems were more important than dispersion or hydrophobic effects for promoting stacking of aromatic molecules. In the case of perfect HOPG, such partial charges would not be present, and only dispersion forces would be expected. Near a defect, however, asymmetry would result in partial charges near the edges and should yield electrostatic interactions with the polar quinones. Such interactions would be enhanced by any oxides present at the step edge. On the basis of the current results, the most likely mechanism for quinone adsorption is an electrostatic interaction with partially charged carbon atoms near the step edge.

The distortion of the STM image near steps could result from several phenomena. It could be rotation of the upper layer relative to the lower, thus modifying the interlayer interaction.[26] This is unlikely for the images of Figure 5, since the upper and lower layers are in registry at points distant from the step edge, as would be expected for a two-layer step on an ABAB ... material. It is possible that the upper layer has delaminated slightly, but that is inconsistent with observation of the observed 0.3 nm layer-to-layer spacing. Partial oxidation or contamination of the defect region by air could occur but should not yield a step height equal to an integral number of graphite layers.

Changes in the STM images of HOPG near defects have been reported by others.[21] A $\sqrt{3} \times \sqrt{3}$ periodicity (0.43 nm) has been previously observed by STM near HOPG

(22) Bansal, R. C.; Donnet, J.-B.; Stoeckli, F. *Active Carbon*, Dekker: New York, 1988; Chapter 4.
(23) Arnett, E. M.; Hutchinson, B. J.; Healy, M. H. *J. Am. Chem. Soc.* **1988**, *110*, 5255.
(24) Chen, S-H.; McGuffin, V. L. *Appl. Spectrosc.* **1994**, *116*, 596.
(25) Newcomb, L. F.; Gellman, S. H. *J. Am. Chem. Soc.* **1994**, *116*, 4993.
(26) (a) Liu, C. Y.; Chang, H.; Bard, A. J. *Langmuir* **1991**, *7*, 1138. (b) Buckley, J. E.; Wragg, J. L.; White, H. W.; Bruckdorfer, D. L.; Worcester, D. L. *J. Vac. Sci. Technol. B* **1991**, *9*, 1079.

surface features such as implanted Ar atoms,[21a] platinum particles,[21b] grain boundaries,[21c] holes,[21d] adsorbates,[21e] as well as step edges.[7b,d,21f] This structure has been shown to occupy a significant area near these surfaces features. Mizes and Foster postulated that the $\sqrt{3} \times \sqrt{3}$ structure is not due to a physical rearrangement of atoms but is caused by a defect-induced variation in the electron density at the Fermi energy of the surface atoms.[21e] They also showed that this effect was long range, extending away from the defect. The $\sqrt{3} \times \sqrt{3}$ structure has also been ascribed to an interference of electron waves scattered at the step.[21f]

Several other experimental reports have considered changes in the electronic structure of HOPG due to defects.[27] UPS[27a] and X-ray absorption[27b] observations indicate changes in electron binding energy when HOPG is damaged with energetic argon ions. Riehl et al.[27c] observed surface-sensitive electronic states on HOPG using inverse photoemission and tunneling spectroscopy and attributed these states to defects. It is quite reasonable to conclude that a change in electron density or surface DOS accompanies a defect.

Theoretical studies concerned with the effect of HOPG surface defects on STM images have also appeared in the literature.[28] Soto proposed that a vacancy in the graphite lattice exhibits a higher electron density than the surrounding undamaged region.[28a] A step edge can be considered a long row of vacancies, and one would expect a substantial local perturbation of the surrounding electronic structure. Recently, Kobayashi performed a first-principles band calculation on a stepped graphite surface and predicted the existence of a localized state near the step.[28b] This leads to a sharp increase in the surface density of states (SDOS) at the Fermi energy at the step, as discussed elsewhere.[4] By analogy to disordered semiconductors, Spain has predicted the appearance of localized states in the region of the Fermi energy in disordered graphite, accompanied by an increase in the DOS.

The STM images of fractured GC show a disordered surface compared to HOPG. The accepted model for GC is a structure consisting of small intertwined regions of basal and edge plane.[29] However, our results, as well as those of two previous atomic scale studies of GC, do not reveal any pattern comparable to that of edge plane or of ordered basal plane.[30,31] The data from our STM investigation of GC concludes that 10% of the GC surface exhibits order characterized by a periodicity of 0.29 nm. The high degree of disorder at GC electrodes correlates with monolayer quinone adsorption.

We had concluded previously that the quinones studied do not adsorb on HOPG unless defects are present. The current results show that the quinones studied cover 23–49 times the area of edge plane on HOPG and saturate the entire GC surface. In light of this discrepancy, we now propose that for HOPG electrodes the adsorbates interact with the electronic perturbation caused by the edge, in addition to the edge itself. Since the perturbation is at least 8 times larger than the edge, the perturbed area is more quantitatively consistent with the observed quinone adsorption. In addition, a surface which is entirely disordered electronically would be expected to exhibit saturation coverage, as is the case for GC. This proposition is fundamentally different from an interaction based solely on edge adsorption, since it involves an electronic interaction with the perturbed basal plane or GC surface rather than any specific interaction between edge sites and adsorbate.

The correlation of the large extent STM-observable electronic perturation and the anomalously high adsorption raises the question of cause and effect. The observations are consistent with the conclusion that the electronic pertubation near a step edge leads to partial charges in the HOPG, which attract the quinones. Consistent with the conclusions of Newcomb and Gellman for small aromatic molecules,[25] these electrostatic interactions are more important than dispersion interactions or hydrophobic effects.

Given the current findings plus recent kinetic results, we should reconsider the definition of the word "site" at carbon electrodes. The traditional meaning based on functional groups or a particular edge plane geometry is certainly valid for specific chemical interactions such as chemisorption and electrocatalysis. However, for many outer-sphere electron transfer reactions,[4] and now for quinone adsorption, the "site" must include a defect-induced electronic perturbation of the surface. In these cases, it is not the edge itself that promotes charge transfer and adsorption, but rather the electronic disorder and partial charges caused by the step edge.

Acknowledgment. This work was supported by The Air Force Office of Scientific Research and The National Science Foundation. M.T.M. acknowledges an Amoco Foundation Doctoral Fellowship. The authors appreciate the useful comments of Victoria McGuffin, as well as a preprint of ref 24. Valuable discussions with Edward Arnett are also acknowledged.

(27) (a) Schlogl, R. *Surf. Sci.* **1987**, *189*, 861. (b) Atamny, F.; Blocker, J.; Henschke, B.; Schlogl, R.; Schedel-Niedrig, T.; Bradshaw, A. M. *J. Phys. Chem.* **1992**, *96*, 4522. (c) Reihl, B.; Gimzewski, J. K.; Nicholls, J. M.; Tosatti, E. *Phys. Rev. B* **1986**, *33*, 5770.

(28) (a) Soto, M. *Surf. Sci.* **1990**, *225*, 190. (b) Kobayashi, K. *Phys. Rev. B* **1993**, *48*, 1757.

(29) Jenkins, G. M.; Kawamura, K. *Nature* **1971**, *231*, 175.

(30) (a) Elings, V.; Wudl, F. *J. Vac. Sci. Technol. A* **1988**, *6*, 412. (b) Brown, N. M.; You, H. X. *J. Mater. Chem.* **1991**, *1*, 469.

(31) Brown and You[30b] reported an atomic arrangement for a polished GC surface which corresponds to a $\sqrt{3} \times \sqrt{3}$ graphitic structure. However, because of their surface preparation and material synthesis, direct comparison to this work is questionable.